Accepted version on Author's Personal Website: C. R. Koch

Article Name with DOI link to Final Published Version complete citation:

K. Ebrahimi, Alexander Schramm, and C. R. Koch. Feedforward/feedback control of HCCI combustion timing. In *2014 American Controls Conference (ACC), Portland, USA*, page 6, June 2014

See also:

https://sites.ualberta.ca/~ckoch/open_access/Ebrahimi_acc2014.pdf

Accepted

As per publisher copyright is ©2014

This work is licensed under a
Creative Commons Attribution-NonCommercial-NoDerivatives 4.0 International License.

Article accepted version starts on the next page ⟶

Or link: to Author's Website

2014 American Control Conference (ACC)
June 4-6, 2014. Portland, Oregon, USA

Feedforward/Feedback Control of HCCI combustion timing

Khashayar Ebrahimi, Alexander Schramm and Charles Robert Koch

Abstract— **Homogeneous Charge Compression Ignition (HCCI) engines have the advantage of low Nitrogen Oxides (NO_x) and soot emissions. In HCCI engines, a lean premixed air-fuel mixture is compressed until the temperature is high enough for combustion to occur. HCCI engines have a limited operating range and are limited by knock at high loads and misfire at low loads. They are without a direct source to initiate ignition so HCCI requires combustion timing control. Some of the factors that affect HCCI combustion timing are mixture composition, pressure and temperature at the time of inlet valve closing. One effective way to control HCCI combustion timing is Variable Valve Timing (VVT). VVT changes the amount of trapped residual gas and the effective compression ratio. These factors have a strong effect on HCCI combustion timing. One main advantage of VVT is that it is fast enough to handle rapid transients. Based on a simplified control oriented model that models the effect of trapped residual gas on combustion timing, a Feedforward/Feedback controller is designed for HCCI combustion timing control . The controller requires feedforward information of the valve timing and feedback information of the combustion timing. This controller tracks the desired combustion timing trajectory both in simulation and experiment by modulating the trapped residual gas using VVT actuation.**

I. INTRODUCTION

HCCI engines have the potential of simultaneously reducing pollutant emissions and fuel consumption [1]. In HCCI engines, a lean homogenous air-fuel mixture is compressed until the entire mixture auto-ignites. Since HCCI combustion temperature is low, unburned hydrocarbons and carbon monoxide emissions can be high and exhaust after-treatment is needed [1]. There is no direct mechanism for combustion timing control in HCCI engines. To get the desired HCCI combustion timing, the mixture temperature, pressure and composition at Inlet Valve Closing (IVC) must be controlled. Different methods have been used for HCCI combustion timing control such as: exhaust gas recirculation (EGR) [2]; intake air heating [3]; variable valve timing [4]; variable compression ratio [5] and dual-fuel [6]. Amongst them, VVT seems promising since it changes the amount of trapped hot residual gases inside the cylinder quickly (cycle by cycle) and a precise mixture at IVC can be realized.

Several control strategies have been developed for HCCI combustion timing control using VVT. A PI controller is implemented in a single cylinder research engine for combustion timing control where the amount of trapped residual gas mass is varied using the negative valve overlap duration [7]. A baseline controller is used for combustion timing control by changing valve and fuel injection timing and a reference governor is added to modify the fuel injection amount while considering actuator constraints [8]. Model predictive control, which consists of a physics based model that uses valve timing and fuel injection as inputs is designed for combustion timing control [4]. Model predictive control, based on a model obtained by system identification, is described in [9]. VVT and dual fuel strategies are used for combustion timing and load control with simultaneous minimization of the fuel consumption and emissions. A physics based control oriented model is developed for both in-cylinder pressure and combustion timing control [10]. A H_2 optimal controller based on the linearized model is implemented on a single-cylinder research engine. A layered control strategy for combustion timing and load control by combining PID and feed forward control is implemented in [11]. An adaptive controller using a Re-Breathing Lift technique is developed to keep ignition timing constant in the presence of uncertainties in runner wall temperature and cylinder charge properties [12]. The controller is based on a simplified bilinear parametric model in which the parameters are updated by feedback information of the cycle by cycle combustion timing.

However, much improvement is still needed to obtain smooth and fast HCCI combustion timing control using VVT. In this work, a Feedforward/Feedback (Fdfwd/Fdbk) controller is developed for HCCI combustion timing control on a single cylinder research engine with valve timing as the actuator. Similar to [7], symmetric Negative Valve Overlap (NVO) is used as a variable valve timing strategy in which the exhaust valves are closed before top dead center (TDC) of the exhaust stroke and the intake valves are opened after TDC of the same stroke. The controller is based on a model that relates combustion timing to the valve timing in feedforward and combustion timing is used as feedback to zero the steady state error using a constant gain integrator (see figure 2). The controller algorithm is first tested in simulation on a detailed phyiscal model and then is implemented on a single cylinder research engine where the results show that combustion timing is tracked accurately for commanded step changes in combustion timing.

II. CONTROL ORIENTED MODEL

A physical model is developed for HCCI combustion timing prediction. The model includes induction, mixing, compression and combustion processes. The model inputs are intake manifold pressure and temperature, fueling rate, engine speed and valve timing and the model output is combustion timing. The crank angle at which 50% of the

K. Ebrahimi, A. Schramm and C. R. Koch are with the Department of Mechanical Engineering, University of Alberta, Edmonton, AB, T6G 2G8 , Canada (e-mail: ebrahimi@ualberta.ca, schramm@ualberta.ca; bob.koch@ualberta.ca).

energy is released, θ_{50}, is used as an indicator for combustion timing [13], [14]. Fueling rate and engine speed variations are considered disturbances to the plant. The model is developed for n-heptane fuel and can be easily reformulated for other fuels since it is parameterized by a Detailed Physical Model (DPM) [15].

Mixture temperature at IVC is determined first since it has an important effect on HCCI combustion timing. It is assumed that the inducted premixed air fuel is mixed with the trapped residual from the previous cycle instantaneously at the instant of IVC. Mixture temperature at IVC is calculated as:

$$T_{IVC} = \frac{\lambda m_{fuel} L_{st} c_{p,air} T_{int} + \frac{P_{em} V_{EVC}}{R_{resid}} c_{p,resid} + m_{fuel} c_{p,fuel} T_{fuel}}{\lambda m_{fuel} L_{st} c_{p,air} + m_{fuel} c_{p,fuel} + \frac{P_{em} V_{EVC}}{R_{resid} T_{em}} c_{p,resid}} \quad (1)$$

and the residual gas mass fraction is calculated from:

$$x_{resid} = \frac{\frac{P_{em} V_{EVC}}{R_{resid} T_{em}}}{\frac{P_{em} V_{EVC}}{R_{resid} T_{em}} + m_{fuel} + \lambda m_{fuel} L_{st}} \quad (2)$$

A simplified integrated Arrhenius model [16], [17] is used for HCCI combustion timing simulation and for n-heptane it is [18]:

$$K_{th} = \int_{IVC}^{SOC} \frac{A exp\left(\frac{-E_a}{R_u T_{TDC}}\right) [C_7H_{16}]_{TDC}^{a} [O_2]_{TDC}^{b}}{\omega} d\theta \quad (3)$$

where ω is the engine speed and the parameters A, $\frac{Ea}{Ru}$, a and b are empirical constants determined from literature [16], [18] and are listed in Table I. Oxygen and fuel concentrations at TDC are determined from:

$$[O_2]_{TDC} = \frac{0.0073 m_{air}}{V_{TDC}} \quad (4)$$

$$[C_7H_{16}]_{TDC} = \frac{m_{fuel}}{100 V_{TDC}} \quad (5)$$

where V_{TDC} is the in-cylinder volume at TDC and m_{air} is calculated as:

$$m_{air} = \lambda m_{fuel} L_{st} \quad (6)$$

and L_{st} is 15.1 for n-heptane.

Substituting equations 4 and 5 into equation 3, the Start of Combustion (SOC), θ_{SOC}, is calculated as:

$$\theta_{SOC} = \theta_{IVC} + \frac{\omega K_{th} exp\left(\frac{E_a}{R_u T_{TDC}}\right)}{A\left(\frac{m_{fuel}}{100 V_{TDC}}\right)^{a} \left(\frac{0.0073 m_{air}}{V_{TDC}}\right)^{b}} + \theta_{Offset} \quad (7)$$

DPM simulations at over 150 engine operating points between $2 \leq \lambda \leq 3$ and $40 \leq NVO \leq 120$ are used to parameterize θ_{offset} and K_{th} and are listed in Table I. These values are obtained by minimizing the difference between θ_{SOC} from the DPM and equation 7. In equation 7, T_{TDC} is calculated assuming isentropic compression as:

$$T_{TDC} = \left(\frac{V_{IVC}}{V_{TDC}}\right)^{\gamma - 1} T_{IVC} \quad (8)$$

where γ is the heat capacity ratio of the trapped mixture. It is also assumed that once the predetermined threshold, K_{th}, in equation 7 is exceeded, the combustion process is initiated. Combustion duration, $\Delta\theta$, is calculated based on the correlation [19] as:

$$\Delta\theta = C(1 + x_{resid})^{D} \lambda^{E} \quad (9)$$

where C, D, and E are constants which are determined from experimental data and are listed in Table I. Finally, θ_{50} is calculated as:

$$\theta_{50} = \theta_{SOC} + 0.5\Delta\theta \quad (10)$$

TABLE I
MODEL PARAMETERS

A	4.63×10^{11}
$\frac{Ea}{Ru}$	15098 [K]
a	0.25
b	1.5
K_{th}	2.3×10^{-6}
θ_{offset}	2.9613 [rad]
C	6.72
D	0.25
E	-0.12

III. CONTROLLER STRUCTURE

The controller uses θ_{50} as feedback and adjusts the trapped residual gas mass fraction with EVC and IVO timing for combustion timing control. Measured cylinder pressure is used to determine θ_{50} [20]. However, combustion timing is needed as a function of in-cylinder volume at EVC. First, λ that appears in equations 2, 6 and 7, is written as a function of in-cylinder volume at EVC:

$$\lambda = 0.0662 \frac{\eta_v P_{int} (V_{IVC} - V_{EVC})}{R_{int} T_{int} m_{fuel}} \quad (11)$$

where volumetric efficiency (η_v) is calculated as in [21]. Substitution of equations 9, 2, 7 and 11 into equation 10, results in combustion timing (θ_{50}) expressed as a function of in-cylinder volume at EVC as:

$$\theta_{50} = \frac{\omega K_{th}}{A} \times exp\left(\frac{E_a R_u^{-1} \left(\frac{V_{IVC}}{V_{TDC}}\right)^{1-\gamma}}{\frac{\frac{\eta_v P_{int} (V_{IVC} - V_{EVC})}{R_{int}} c_{p,air} + \frac{P_{em} V_{EVC}}{R_{resid}} c_{p,resid} + m_{fuel} c_{p,fuel} T_{fuel}}{\frac{\eta_v P_{int} (V_{IVC} - V_{EVC})}{R_{int} T_{int}} c_{p,air} + m_{fuel} c_{p,fuel} + \frac{P_{em} V_{EVC}}{R_{resid} T_{em}} c_{p,resid}}} \right) \Bigg/ \left(\frac{m_{fuel}}{100 V_{TDC}}\right)^{a} \left(\frac{0.0073 \frac{\eta_v P_{int} (V_{IVC} - V_{EVC})}{R_{int} T_{int}}}{V_{TDC}} \right)^{b}$$

$$+ 0.5C \left(1 + \frac{\frac{P_{em} V_{EVC}}{R_{resid} T_{em}}}{\frac{P_{em} V_{EVC}}{R_{resid} T_{em}} + m_{fuel} + \frac{\eta_v P_{int} (V_{IVC} - V_{EVC})}{R_{int} T_{int}}} \right)^{D} \times \left(0.0662 \frac{\eta_v P_{int} (V_{IVC} - V_{EVC})}{R_{int} T_{int} m_{fuel}} \right)^{E} + \theta_{IVC} + \theta_{Offset} \quad (12)$$

Given a desired θ_{50}, it is difficult to solve equation 12 for V_{EVC} so Trust Region Reflective Algorithm [22] is used for solving this equation. EVC timing is determined from slider crank mechanism [23] equation using V_{EVC} from equation 12 as:

$$V_{EVC} = V_c + \frac{\pi B^2}{4}[l + a - a\cos\theta_{EVC} - \sqrt{l^2 - (a\sin\theta_{EVC})^2}] \tag{13}$$

V_c is the cylinder clearance volume, B is the cylinder bore, l is the connecting rod length and $L = 2a$ is the stroke. The IVO timing is

$$\theta_{IVO} = -\theta_{EVC} \tag{14}$$

since symmetric negative valve overlap is implemented. A constant gain discrete time integrator is used to zero the steady error as:

$$u_k = u_{k-1} + k_i T e_k \tag{15}$$

$$\theta_{EVC,k} = \theta_{EVC,k-1} + u_k \tag{16}$$

$$\theta_{IVO,k} = \theta_{IVO,k-1} - u_k \tag{17}$$

where e = $\theta_{50}(Ref) - \theta_{50}$(Meas) is the error and T, k and k_i are the sample time, cycle number, and integral gain respectively (k_i = 3 is tuned while $\theta_{EVC,1}$ and $\theta_{IVO,1}$ are calculated from equations 13 and 14). For realtime implementation on the engine, equations 12 and 13 are solved for different desired combustion timings and fueling rates and the values are tabulated in a lookup table. This linear interpolation lookup table is used to reduce processing time. The lookup table is shown in Figure 1 and the controller structure is shown in Figure 2.

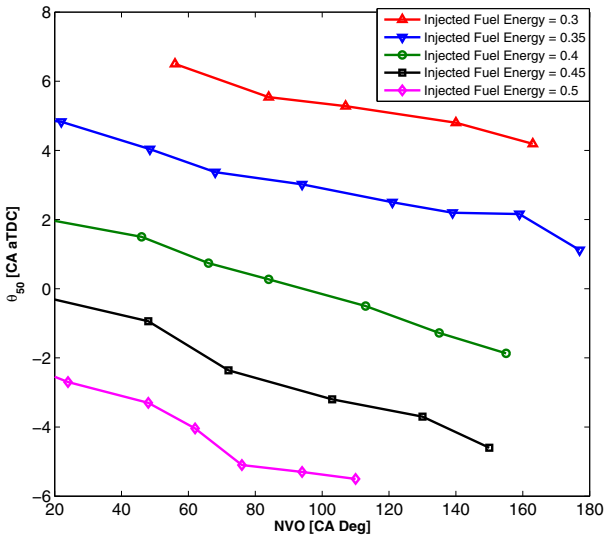

Fig. 1. The implemented lookup table [n = 825 RPM]

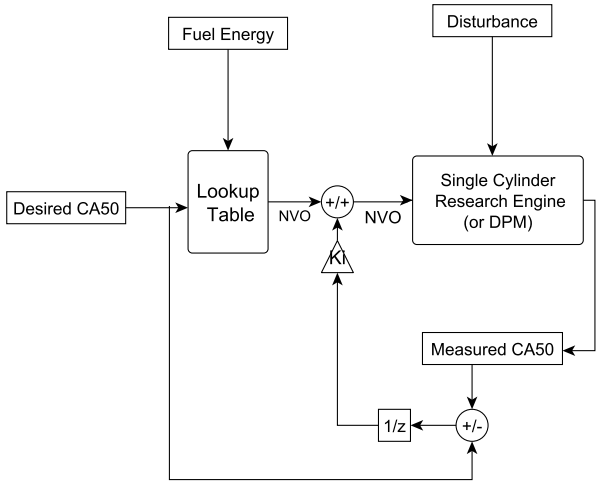

Fig. 2. Controller structure

IV. Model Validation

First, the model is validated on a single cylinder research engine (specifications listed in Table II). Both steady-state and transient performance of the model are tested by comparing predicted θ_{50} to experiments. The test points used here for model validation have not been used for model parametrization.

TABLE II
SINGLE CYLINDER RESEARCH ENGINE SPECIFICATIONS [24]

Bore [mm]	97
Stroke [mm]	88.9
Compression ratio [-]	13.9:1
Connecting rod length [mm]	159
Rated Speed [RPM]	823±12
IVO [CA deg bTDC]	280
IVC [CA deg bTDC]	180
EVO [CA deg bTDC]	-180
EVC [CA deg bTDC]	-280

For steady state validation, fueling rate is kept constant and the NVO duration is varied. Figure 3 shows θ_{50} versus the NVO duration for two different fueling rates. As shown in this figure, model accuracy is sufficient for control purposes. The difference between measured and the predicted combustion timing is attributed to the assumptions used in the Arrhenius integral simplification. In-cylinder residual gas mass fraction increases when NVO timing increases causing mixture temperature at IVC to increase and the combustion timing to advance. The model is further validated by holding the valve timing constant while varying the fueling rates. Figure 4 shows the variation of θ_{50} with respect to λ for two different NVOs. The reactivity of the mixture tends to increase from lean to rich conditions.

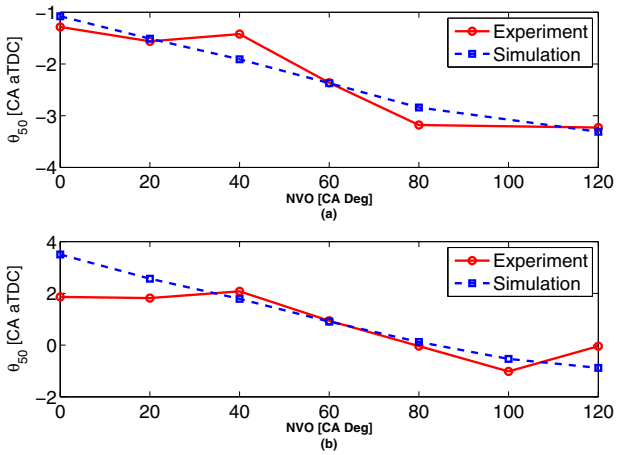

Fig. 3. Comparison of predicted and measured θ_{50} for NVO variation (a) Injected Fuel Energy = 0.46 kJ, (b) Injected Fuel Energy = 0.39 kJ [n = 791 RPM]

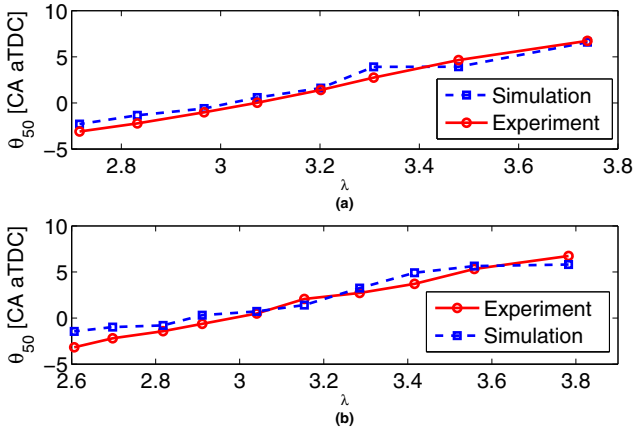

Fig. 4. Comparison of predicted and measured θ_{50} for λ variation (a) NVO= 100° CA (b) NVO= 40° CA [n=791 RPM]

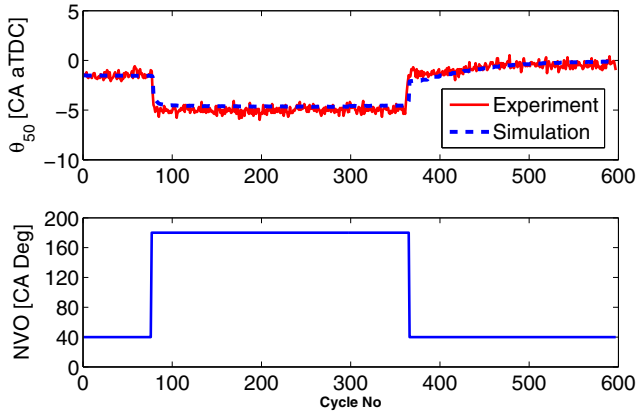

Fig. 5. NVO duration step: Comparison between predicted and measured θ_{50} [n=788 RPM, and Injected fuel energy=0.45 kJ]

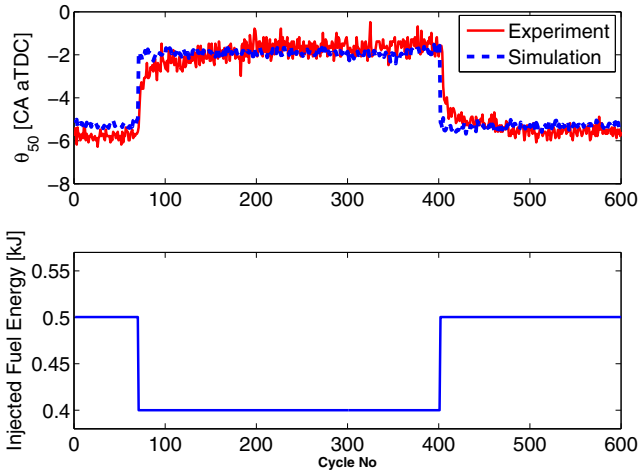

Fig. 6. Fueling rate step: Comparison between predicted and measured θ_{50} [n=791 RPM, NVO=120 CA Deg]

The transient response to steps in NVO are shown in Figure 5. As expected, θ_{50} advances when NVO duration increases. The resulting θ_{50} of the model and engine are plotted showing that the model captures the transient dynamics quite accurately. Experimental and simulated combustion timing for transient fueling rate are compared in Figure 6. The simulation model reaches the final value earlier compared to the experimental data since the fuel transport dynamics [19] are not considered in the model. Predicted θ_{50} is in good agreement with the experiment and the model captures the overall dynamic trend of changes in fueling rate sufficiently accurately for control purposes.

V. Controller Performance

Combustion timing (θ_{50}) as measurement and valve timing (EVC, IVO) as inputs to vary the amount of the residual gas in the cylinder of the engine are used for cycle by cycle combustion timing control. Symmetric Negative Valve Overlap duration (NVO) is one effective way to control the in-cylinder temperature and residual gas amount at IVC [17]. A Detailed Physical Model from [15] is used to test and tune the performance of the controller using simulation. The tracking performance of the controller is studied first. Then the disturbance rejection properties of the controller are evaluated for step changes in the engine speed and load. The controller performance is also compared to the manually tuned PI controller [7]. Figure 7 shows the controller tracking performance for θ_{50} set point changes. Both the PI and Fdfwd/Fdbk controllers track the desired trajectory with no steady state error but the new Fdfwd/Fdbk controller has less overshoot. The effect of measurement noise on the tracking performance of both controllers is studied by adding a Gaussian noise with standard deviation of 1.2 CAD to the measured θ_{50} starting at cycle 55 (see Figure 7). The noise level is chosen based on noise levels in typical experimental data. The Fdfwd/Fdbk controller has less oscillations than

the manually tuned PI controller when there is measurement noise. The disturbance rejection of the Fdfwd/Fdbk controller is tested for positive and negative step changes in Figures 8 and 9 in simulation. The Fdfwd/Fdbk controller rejects disturbance from the engine speed and engine load by maintaining θ_{50} within 1 crank angle degree.

The Fdfwd/Fdbk controller is experimentally tested

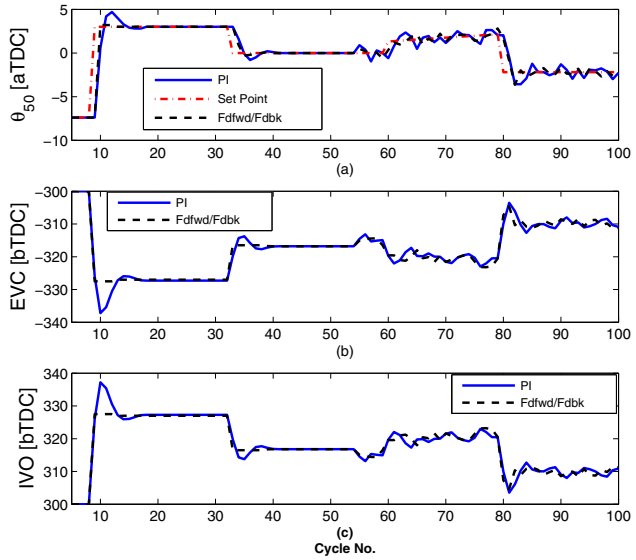

Fig. 7. Tracking performance of the manually tuned PI and feedforward/feedback controllers (a) θ_{50} as controller output (b and c) Controller Inputs [n= 850 RPM, Injected Fuel Energy=0.5 kJ]

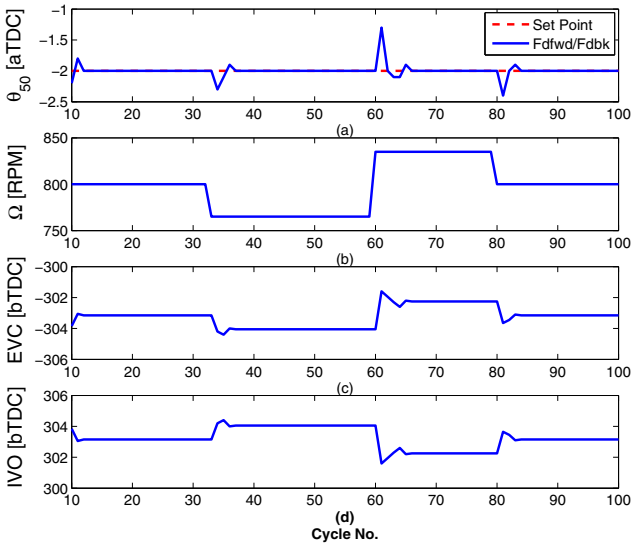

Fig. 8. Disturbance rejection: Engine speed (a) θ_{50} as controller output (b) Disturbance (c and d) Controller Inputs

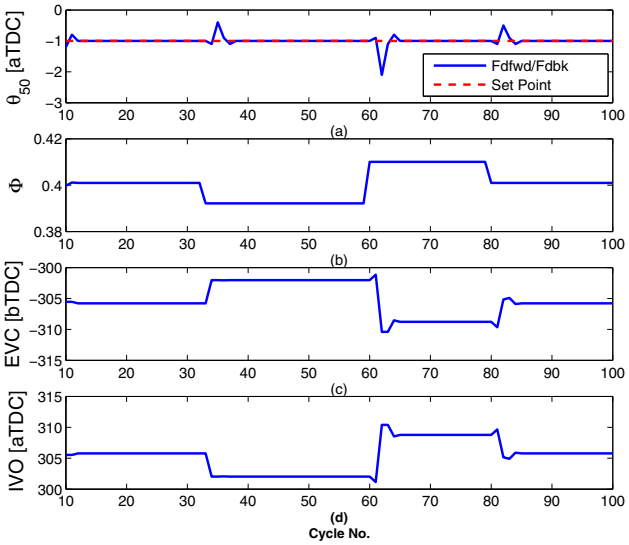

Fig. 9. Disturbance rejection: Engine load (a) θ_{50} as controller output (b) Disturbance (c and d) Controller Inputs

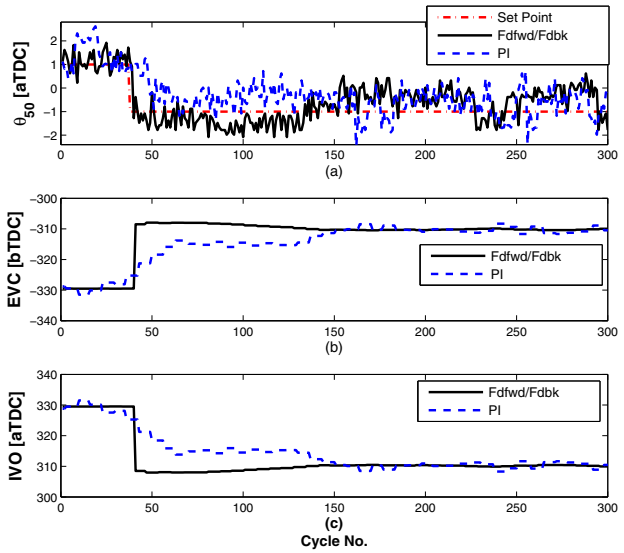

Fig. 10. Tracking performance of the manually tuned PI and feedforward/feedback controllers (step down) (a) θ_{50} as controller output (b and c) Controller Inputs[n= 788 RPM, Injected Fuel Energy=0.4 kJ]

and compared to the PI controller in simulation for step changes in desired combustion timing θ_{50}. First the desired combustion timing is advanced by two degrees (see Figure 10) and then it returned back to its original value (see figure 11). Both controllers track the desired trajectory but the Fdfwd/Fdbk controller has faster response and smoother tracking performance in both cases. The Fdfwd/Fdbk showed similar improvements over the PI controller at other fueling rates.

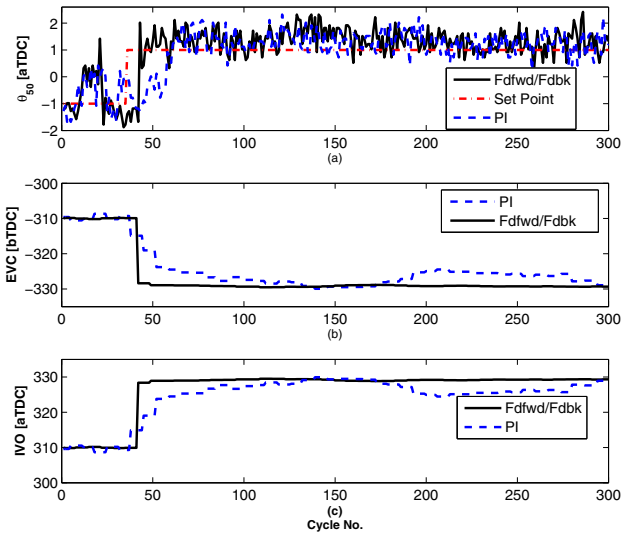

Fig. 11. Tracking performance of the manually tuned PI and feedforward/feedback controllers (step up) (a) θ_{50} as controller output (b and c) Controller Inputs [n= 788 RPM, Injected Fuel Energy=0.4 kJ]

VI. CONCLUSIONS

A Fdfwd/Fdbk controller that controls HCCI combustion timing (θ_{50}) by varying valve timing cycle-by-cycle is developed using a detailed engine model and validated on a single cylinder engine. Performance of the new controller is compared to a PI controller developed in a previous study [7] and the results show that the Fdfwd/Fdbk controller performance has improved tracking of the desired combustion timing and performs well in maintaining a desirable engine combustion timing during load and engine speed disturbances.

REFERENCES

[1] H. Zhao, *HCCI and CAI engines for the automotive industry*. CRC Press, 2006.

[2] X. C. Lu, W. Chen, and Z. Huang, "A fundamental study on the control of the HCCI combustion and emissions by fuel design concept combined with controllable EGR. part 2. effect of operating conditions and EGR on HCCI combustion," *Fuel*, vol. 84, no. 9, pp. 1084 – 1092, 2005.

[3] Z. C. Hua, P. J. Ru, T. J. Juan, and L. Jing, "Effects of intake temperature and excessive air coefficient on combustion characteristics and emissions of HCCI combustion," *Procedia Environmental Sciences*, vol. 11, Part C, no. 0, pp. 1119 – 1127, 2011.

[4] N. Ravi, H.-H. Liao, A. F. Jungkunz, A. Widd, and J. C. Gerdes, "Model predictive control of HCCI using variable valve actuation and fuel injection," *Control Engineering Practice*, vol. 20, no. 4, pp. 421 – 430, 2012.

[5] M. Christensen, A. Hultqvist, and B. Johansson, "Demonstrating the multi fuel capability of a Homogeneous Charge Compression Ignition Engine with variable compression ratio," SAE Technical paper 1999-01-3679.

[6] R. K. Maurya and A. K. Agarwal, "Experimental investigation of close-loop control of HCCI engine using dual fuel approach," SAE Technical paper 2013-01-1675.

[7] K. Ebrahimi and C. R. Koch, "HCCI combustion timing control with variable valve timing," in *American Control Conference (ACC), 2013*, 2013, pp. 4429–4434.

[8] S. Jade, J. Larimore, E. Hellstrom, L. Jiang, and A. G. Stefanopoulou, "Enabling large load transitions on multicylinder recompression HCCI engines using fuel governors," in *American Control Conference (ACC), 2013*, 2013, pp. 4423–4428.

[9] J. Bengtsson, P. Strandh, R. Johansson, P. Tunestal, and B. Johansson, "Multi-output control of a heavy duty HCCI engine using variable valve actuation and model predictive control," SAE Technical papaer 2006-01-0873.

[10] G. M. Shaver, J. C. Gerdes, M. J. Roelle, P. A. Catton, and F. E. Christopher, "Dynamic modeling of residual-affected Homogeneous Charge Compression Ignition Engines with variable valve actuation," *Journal of Dynamics System, Measurement, and Control*, vol. 127, pp. 374 –381, 2005.

[11] N. Zhou, H. Xie, N. Li, T. Chen, and H. Zhao, "Study on layered close-loop control of 4-stroke gasoline HCCI engine equipped with 4VVAS," SAE Technical paper 2008-01-0791.

[12] C. J. Chiang, C. C. Chou, and J. H. Lin, "Adaptive control of homogeneous charge compression ignition (HCCI) engines," in *American Control Conference (ACC), 2012*, 2012, pp. 2066–2071.

[13] A. Widd, P. Tunestal, and R. Johansson, "Physical modeling and control of Homogeneous Charge Compression Ignition (HCCI) engines," in *Decision and Control, 2008. CDC 2008. 47th IEEE Conference on*, 2008, pp. 5615–5620.

[14] N. J. Killingsworth, S. M. Aceves, D. L. Flowers, F. Espinosa-Loza, and M. Krstic, "HCCI engine combustion-timing control: Optimizing gains and fuel consumption via extremum seeking," *Control Systems Technology, IEEE Transactions on*, vol. 17, no. 6, pp. 1350–1361, 2009.

[15] K. Ebrahimi, C. R. Koch, and A. Schramm, "A control oriented model with variable valve timing for HCCI combustion timing control," SAE Technical paper 2013-01-0588.

[16] J. B. Bettis, J. A. Massey, J. A. Drallmeier, and J. Sarangapani, "A thermodynamics-based Homogeneous Charge Compression Ignition Engine model for adaptive nonlinear controller development," *Proceedings of the Institution of Mechanical Engineers, Part D: Journal of Automobile Engineering*, vol. 226, no. 11, pp. 1547–1563, 2012.

[17] G. M. Shaver, "Physics-based modeling and control of residual-affected HCCI engines using variable valve actuation," Ph.D. dissertation, Stanford University, 2005.

[18] S. Turns, *An introduction to combustion : concepts and applications*. New York: McGraw-Hill, 2012.

[19] M. Shahbakhti and C. R. Koch, "Dynamic modeling of HCCI combustion timing in transient fueling operation," pp. 1098–1113, SAE Technical paper 2009-01-1136.

[20] M. Wenig, M. Grill, and M. Bargende, "Fundamentals of pressure trace analysis for gasoline engines with Homogeneous Charge Compression Ignition," SAE Technical paper 2010-01-2182.

[21] L. Kocher, E. Koeberlein, D. Van Alstine, K. Stricker, and G. Shaver, "Physically based volumetric efficiency model for diesel engines utilizing variable intake valve actuation." *International Journal of Engine Research*, vol. 13, no. 2, pp. 169 – 184, n.d.

[22] T. Coleman and Y. Li, "An interior trust region approach for nonlinear minimization subject to bounds." *SIAM Journal on Optimization*, vol. 6, no. 2, pp. 418 – 445, n.d.

[23] J. S. Souder, "Closed-loop control of a multi-cylinder HCCI engine," Ph.D. dissertation, University of California, Berkeley, 2004.

[24] R. Seethaler, C. R. Koch, R. Chladny, and M. Mashkournia, "Closed loop electromagnetic valve actuation motion control on a single cylinder engine," SAE Technical paper 2013-01-0594.